© 2014. Published by The Company of Biologists Ltd | The Journal of Experimental Biology (2014) 217, 1830 doi:10.1242/jeb.107326

CORRECTION

Molt regulation in green and red color morphs of the crab *Carcinus maenas*: gene expression of molt-inhibiting hormone signaling components

Ali M. Abuhagr, Jennifer L. Blindert, Sukkrit Nimitkul, Ian A. Zander, Stefan M. LaBere, Sharon A. Chang, Kyle S. MacLea, Ernest S. Chang and Donald L. Mykles

There was an error published in *J. Exp. Biol.* **217**, pp. 796-808.

In Fig. 3, the letters and numbers indicating which means were significantly different are missing from panel A. The correct figure is printed below.

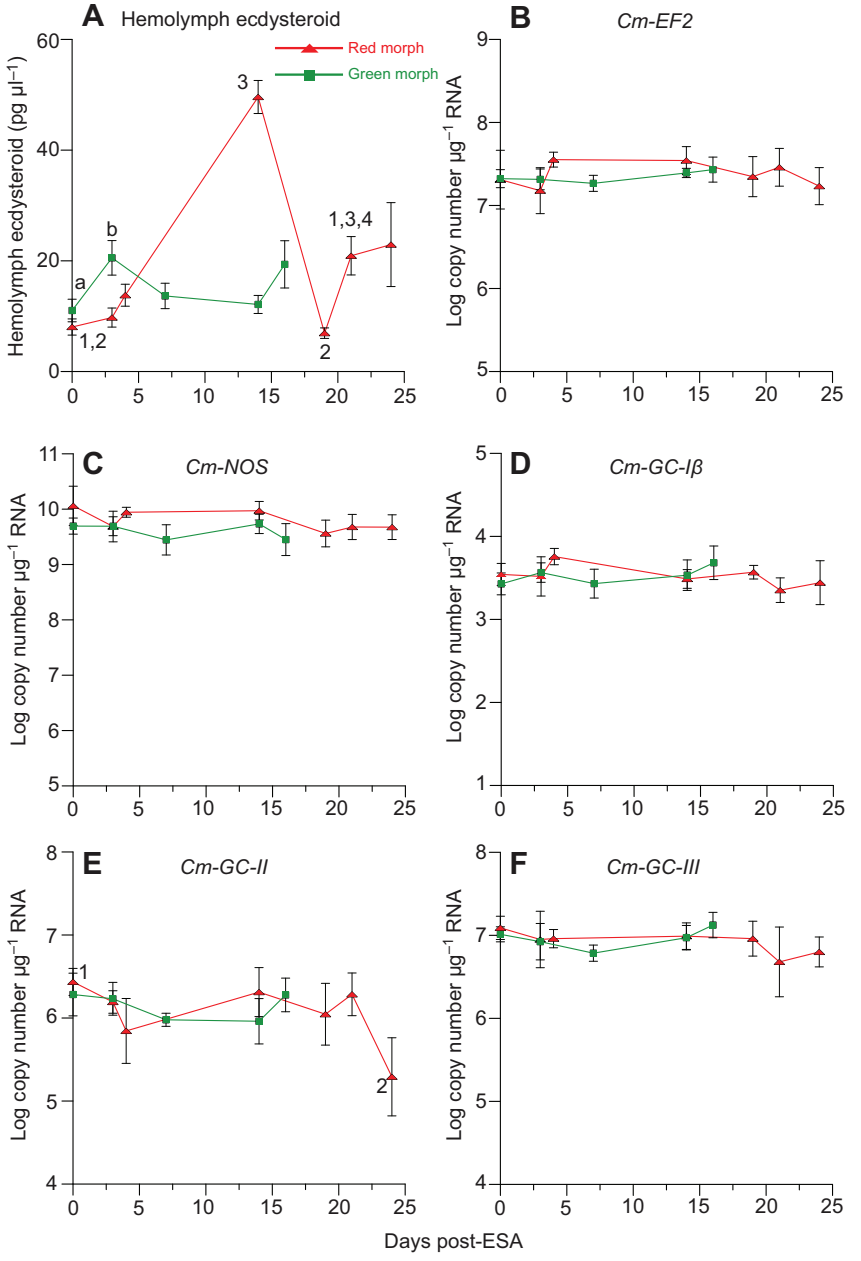

Fig. 3. Effects of eyestalk ablation (ESA) on hemolymph ecdysteroid, nitric oxide synthase (NOS) and guanylyl cyclase expression in red (triangles) and green (squares) morphs over 24 and 16 days, respectively. Animals were eyestalk-ablated at Day 0. YOs were harvested and hemolymph samples were taken at various intervals post-ESA. Ecdysteroid levels were quantified by ELISA. mRNA levels were quantified by qPCR. Data are presented as means ± 1 s.e.m. (red morph, *N*=7, 3, 6 and 3 at Days 0, 3, 14 and 24, respectively; green morph, *N*=13, 5, 5, 5 and 4 at Days 0, 3, 7, 14 and 16, respectively). Different letters (numbers) indicate green (red) morphs that are significantly different ($P<0.05$) from each other.

We apologise to the authors and readers for this omission.

© 2014. Published by The Company of Biologists Ltd | The Journal of Experimental Biology (2014) 217, 796-808 doi:10.1242/jeb.093385

RESEARCH ARTICLE

Molt regulation in green and red color morphs of the crab *Carcinus maenas*: gene expression of molt-inhibiting hormone signaling components

Ali M. Abuhagr[1], Jennifer L. Blindert[1], Sukkrit Nimitkul[2], Ian A. Zander[1], Stefan M. LaBere[1], Sharon A. Chang[2], Kyle S. MacLea[1], Ernest S. Chang[2] and Donald L. Mykles[1,*]

ABSTRACT

In decapod crustaceans, regulation of molting is controlled by the X-organ/sinus gland complex in the eyestalks. The complex secretes molt-inhibiting hormone (MIH), which suppresses production of ecdysteroids by the Y-organ (YO). MIH signaling involves nitric oxide and cGMP in the YO, which expresses nitric oxide synthase (NOS) and NO-sensitive guanylyl cyclase (GC-I). Molting can generally be induced by eyestalk ablation (ESA), which removes the primary source of MIH, or by multiple leg autotomy (MLA). In our work on *Carcinus maenas*, however, ESA has limited effects on hemolymph ecdysteroid titers and animals remain in intermolt at 7 days post-ESA, suggesting that adults are refractory to molt induction techniques. Consequently, the effects of ESA and MLA on molting and YO gene expression in *C. maenas* green and red color morphotypes were determined at intermediate (16 and 24 days) and long-term (~90 days) intervals. In intermediate-interval experiments, ESA of intermolt animals caused transient twofold to fourfold increases in hemolymph ecdysteroid titers during the first 2 weeks. In intermolt animals, long-term ESA increased hemolymph ecdysteroid titers fourfold to fivefold by 28 days post treatment, but there was no late premolt peak (>400 pg μl^{-1}) characteristic of late premolt animals and animals did not molt by 90 days post-ESA. There was no effect of ESA or MLA on the expression of *Cm-elongation factor 2* (*EF2*), *Cm-NOS*, the beta subunit of GC-I (*Cm-GC-Iβ*), a membrane receptor GC (*Cm-GC-II*) and a soluble NO-insensitive GC (*Cm-GC-III*) in green morphs. Red morphs were affected by prolonged ESA and MLA treatments, as indicated by large decreases in *Cm-EF2*, *Cm-GC-II* and *Cm-GC-III* mRNA levels. ESA accelerated the transition of green morphs to the red phenotype in intermolt animals. ESA delayed molting in premolt green morphs, whereas intact and MLA animals molted by 30 days post treatment. There were significant effects on YO gene expression in intact animals: *Cm-GC-Iβ* mRNA increased during premolt and *Cm-GC-III* mRNA decreased during premolt and increased during postmolt. *Cm-MIH* transcripts were detected in eyestalk ganglia, the brain and the thoracic ganglion from green intermolt animals, suggesing that MIH in the brain and thoracic ganglion prevents molt induction in green ESA animals.

KEY WORDS: Arthropoda, Crustacea, Brachyura, Nitric oxide synthase, Guanylyl cyclase, Y-organ, Ecdysteroid, Eyestalk ablation, Autotomy, cDNA cloning, DNA sequence, Amino acid sequence

[1]Department of Biology, Colorado State University, Fort Collins, CO 80523, USA. [2]Bodega Marine Laboratory, University of California, Davis, Bodega Bay, CA 94923, USA.

*Author for correspondence (Donald.Mykles@ColoState.edu)

Received 5 July 2013; Accepted 16 October 2013

INTRODUCTION

Color morphotypes

The European green crab, *Carcinus maenas* (Linnaeus 1758), has invaded coastal and estuarine habitats worldwide from its native range in the eastern North Atlantic (Grosholz and Ruiz, 1996; Hänfling et al., 2011). On the west coast of the USA, *C. maenas* ,were observed in Bodega Bay, California in 1993 and now the harbor sustains a resident population (de Rivera et al., 2011; Grosholz and Ruiz, 1995). Genetic analysis indicates that the populations at Bodega Bay and other western North American coastal locations are derived from a small number of individuals introduced to San Francisco Bay, California, from the east coast of North America (Darling et al., 2008; Grosholz and Ruiz, 1995; Tepolt et al., 2009). Adults occur as two color morphs that are distinguished by the pigmentation of the ventral surface of the thoracic segments and the arthrodial membrane articulating the basal segments of each of the legs (McGaw et al., 1992; McGaw and Naylor, 1992). In the Bodega Harbor population, green morphs are more common during the winter months and molt frequently during December to April. In UK populations, juvenile green morphs molt frequently during the first year and males become sexually mature at 25–30 mm carapace width (CW) (Crothers, 1967). The green morphs transition to red morphs during the summer and are most common in autumn. Adult green morphs direct more energy into molting and growth, while red morphs molt less frequently and direct more energy to reproduction (Reid et al., 1997; reviewed by Styrishave et al., 2004a). In UK populations, animals reach a large size after approximately 18 molts (CW >70 mm) and enter terminal anecdysis, a condition in which the animals no longer molt (Carlisle, 1957; Crothers, 1967).

Control of molting

Molting in crustaceans requires precise coordination of physiological processes occurring in various organs and tissues, such as the degradation of the old exoskeleton, synthesis of a new exoskeleton, regeneration of lost appendages and atrophy of skeletal muscle in the claws (reviewed by Chang and Mykles, 2011; Skinner, 1985). The molt cycle is divided into four major stages: intermolt, premolt, ecdysis and postmolt (Chang and Mykles, 2011; Skinner, 1985). Steroid molting hormones, or ecdysteroids, which are synthesized and secreted by a pair of molting glands, or Y-organs (YOs), initiate and coordinate these processes (reviewed by Lachaise et al., 1993; Skinner, 1985). Thus, the YOs, located in the anterior cephalothorax, are activated to initiate the transition from the intermolt stage to the premolt stage (reviewed by Chang and Mykles, 2011). Hemolymph ecdysteroid levels are low during postmolt and intermolt stages, and increase during premolt, reaching a peak at the end of premolt

The Journal of Experimental Biology

The Journal of Experimental Biology (2014) doi:10.1242/jeb.093385

List of abbreviations

AB	assay buffer
BSA	bovine serum albumin
CHH	crustacean hyperglycemic hormone
CW	carapace width
EF2	elongation factor 2
ELISA	enzyme-linked immunosorbent assay
ESA	eyestalk ablation
GC	guanylyl cyclase
GC-1	NO-sensitive guanylyl cyclase
HRP	horseradish peroxidase
KH	kinase homology
MIH	molt-inhibiting hormone
MLA	multiple leg autotomy
NOS	nitric oxide synthase
NSB	non-specific binding
ORF	open reading frame
PBS	phosphate-buffered saline
PDE	phosphodiesterase
UTR	untranslated region
XO/SG	X-organ/sinus gland
YO	Y-organ
20E	20-hydroxyecdysone

(reviewed by Chang, 1989; Mykles, 2011). There is a large drop in ecdysteroid level a few days before ecdysis, which serves as a trigger for shedding of the exoskeleton (Chang and Mykles, 2011; Skinner, 1985).

The YOs are controlled by inhibitory neuropeptides produced by the X-organ/sinus gland (XO/SG) complex located in the eyestalks of decapod crustaceans (reviewed by Chang and Mykles, 2011; Hopkins, 2012; Lachaise et al., 1993; Skinner, 1985; Webster et al., 2012). Molt-inhibiting hormone (MIH) and crustacean hyperglycemic hormone (CHH) inhibit ecdysteroidogenesis in the YO (reviewed by Chang and Mykles, 2011; Covi et al., 2012; Nakatsuji et al., 2009; Webster et al., 2012). MIH is expressed primarily in the XO/SG complex, but there are reports of MIH mRNA and peptide in extra-eyestalk nervous tissues (Lu et al., 2001; Stewart et al., 2013; Tiu and Chan, 2007; Zhu et al., 2011). By contrast, CHH is expressed in a wide variety of tissues including the XO/SG complex (Webster et al., 2012). Both neuropeptides share similar highly conserved motifs (reviewed by Nakatsuji et al., 2009; Webster et al., 2012) and inhibit ecdysteroid synthesis via cGMP-dependent signaling pathways (reviewed by Covi et al., 2009; Mykles et al., 2010). CHH is a pleiotropic neuropeptide that regulates glucose utilization, molting, osmoregulation and metabolism (reviewed by Chung et al., 2010; Fanjul-Moles, 2006; Webster et al., 2012). The eyestalk CHH isoform inhibits the YO through a membrane receptor guanylyl cyclase, or GC-II (Chung et al., 2010). MIH signaling pathway may involve a calmodulin (CaM)-dependent NO synthase (NOS) and NO-dependent guanylyl cyclase (GC-I) (Chang and Mykles, 2011; Covi et al., 2012; Webster et al., 2012). YOs express NOS, the beta subunit of GC-I (GC-Iβ), a receptor GC (GC-II) and a soluble NO-insensitive GC (GC-III) (Kim et al., 2004; Lee et al., 2007a; McDonald et al., 2011). Thus, CHH and MIH inhibit YO ecdysteroid biosynthesis through two distinct signaling pathways involving membrane receptor and NO-dependent GCs, respectively.

In most decapod crustaceans, molting can be induced by eyestalk ablation (ESA) or by autotomy of at least five walking legs [multiple leg autotomy (MLA)] (reviewed by Chang and Mykles, 2011; Mykles, 2001; Skinner, 1985). ESA removes the primary source of MIH and results in an immediate activation of the YO and an increase in hemolymph ecdysteroid titers (Covi et al., 2010; Lee et al., 2007b; Lee and Mykles, 2006; reviewed by Lachaise et al., 1993). In *Gecarcinus lateralis*, ESA increases *Gl-NOS*, *Gl-GC-Iβ* and *Gl-GC-III* expression in the YO by 7 days post-ESA, which indicates that YOs are responsive to acute withdrawal of eyestalk neuropeptides (Lee et al., 2007b; McDonald et al., 2011). In juvenile (5–25 mm CW) *C. maenas*, ESA or MLA shortens the intermolt interval (Adelung, 1971; Bückmann and Adelung, 1964; Spindler et al., 1974). By contrast, adult (>25 mm CW) *C. maenas* appear to be refractory to ESA, but precocious molts can be triggered by MLA (Saïdi et al., 1994; Skinner and Graham, 1972). ESA has relatively small effects on hemolymph ecdysteroid titer and YO *Cm-NOS* mRNA by 7 days post-ESA (McDonald et al., 2011). These data suggest that *C. maenas* adults differ from *C. maenas* juveniles in response to ESA.

The purpose of this study was to investigate aspects of the regulation of molting in adult *C. maenas* from a recently introduced population in northern California. There are few published reports on the effects of ESA and MLA on adults (Skinner, 1985) and none have investigated possible differences between color morphs. As red morphs molt less frequently than green morphs (Styrishave et al., 2004b), we hypothesized that red morphs would be less responsive to molt induction than green morphs. MLA induces precocious molting (Skinner and Graham, 1972), but the effects of ESA are inconsistent. ESA may (Carlisle, 1957) or may not (Carlisle, 1954; Saïdi et al., 1994; Skinner and Graham, 1972) stimulate molting. As older red morph adults occur in a blocked or terminal anecdysis state (Baghdassarian et al., 1996; Carlisle, 1957; Lachaise et al., 1988; Saïdi et al., 1994; Styrishave et al., 2004a; Styrishave et al., 2004b; Webster, 1986), animals (estimated ages between 1 and 2 years) that were capable of molting were used. The effects of ESA and MLA on the color morphs were determined by measuring hemolymph ecdysteroid levels and YO expression of the three GCs, *Cm-NOS*, and the housekeeping gene *Cm-elongation factor 2* (*EF2*), using quantitative reverse transcription-PCR (RT-PCR or qPCR). Gene expression was also quantified in YOs from intact green morphs undergoing spontaneous molts during the winter/spring molting season. The expression of MIH in brain and thoracic ganglion was determined by nested PCR and qPCR. The results showed that both color morphs are refractory to ESA and MLA and that the brain and thoracic ganglion may serve as secondary sources of MIH.

RESULTS

Cloning and characterization of *C. maenas* GCs

Partial cDNAs encoding three GCs from *C. maenas* were obtained by RT-PCR and RACE (Table 1, Fig. 1). Multiple sequence alignments showed that the deduced amino acid sequences of *Cm-GC-Iβ*, *Cm-GC-II* and *Cm-GC-III* were similar to those of other decapod crustacean and insect GCs (supplementary material Figs S1, S2 and S3, respectively). Cm-GC-Iβ shared 93% amino acid identity with Gl-GC-Iβ, Cm-GC-II shared 54% identity with Gl-GC-II, and Cm-GC-III shared 78% identity with Gl-GC-III. The tissue distribution of *Cm-GC-Iβ*, *Cm-GC-II* and *Cm-GC-III* was determined using end-point RT-PCR. All three GCs were expressed in all the tissues examined; *Cm-GC-III* appeared to show a greater variation in expression level (Fig. 2).

Intermediate-interval experiment: effects of ESA and MLA on hemolymph ecdysteroid and gene expression in YOs from red and green morphs

The effects of ESA on hemolymph ecdysteroid levels and NOS and GC expression were determined in green morphs over a 16-day

The Journal of Experimental Biology (2014) doi:10.1242/jeb.093385

Table 1. Partial cDNAs encoding *Carcinus maenas* guanylyl cyclases

Gene	Accession number	Size (bp)	Domain(s)	Identity to *G. lateralis* GC
Cm-GC-Iβ	JQ911525	1260	HNOBA, catalytic and 3′ UTR	93%
Cm-GC-II	JQ911527	1188	KH and catalytic	54%
Cm-GC-III	JQ911526	1157	Catalytic and 3′ UTR	78%

Cm, *C. maenas*; GC, guanylyl cyclase; HNOBA, heme/NO-binding-associated domain; KH, kinase homology domain; UTR, untranslated region.

interval and red morphs over a 24-day interval. ESA resulted in a transient increase in ecdysteroid titers, but the magnitude and timing differed between the color morphs (Fig. 3A). In red morphs, there was a 4.2-fold increase to 48.9 pg µl^{-1} (P<0.0001) in the ecdysteroid concentration at 14 days post-ESA, which was followed by a 3.8-fold decrease (P<0.0001) at 21 days post-ESA (Fig. 3A). In green morphs, there was a twofold increase to 20.5 pg µl^{-1} (P<0.012) in hemolymph ecdysteroid at 3 days post-ESA, which returned to pre-ESA levels at 7 days post-ESA (Fig. 3A).

ESA had little effect on gene expression in the YOs from both color morphs. There was no significant effect on the expression of *Cm-EF2*, *Cm-NOS*, *Cm-GC-Iβ* or *Cm-GC-III* in either color morph (Fig. 3B,C,D and F, respectively). Expression of *Cm-GC-II* in green morphs was not affected by ESA (Fig. 3E). The only significant effect was a decrease in *Cm-GC-II* mRNA level (P<0.022) at 24 days post-ESA in red morphs (Fig. 3E).

Long-term experiment: effects of ESA and MLA on hemolymph ecdysteroid and gene expression in YOs from red and green morphs

The long-term effects of ESA and MLA were determined on red and green morphs. Red morphs were divided into four treatment groups: intact (control), ESA, MLA and combined ESA+MLA. The experiment was conducted during the summer, after the winter/spring molting season. All the red morphs were in the intermolt stage and remained in the intermolt stage; none of the animals molted during the 3-month duration of the experiment.

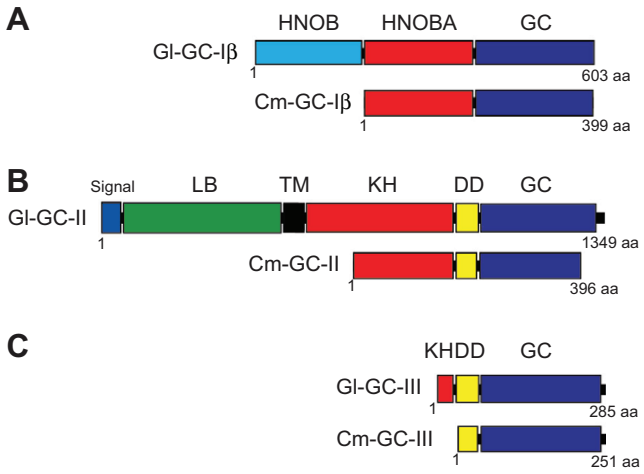

Fig. 1. Domain organization of three guanylyl cyclases from land crab (*Gecarcinus lateralis*; Gl-GC) and green crab (*Carcinus maenas*; Cm-GC). GC-Iβ, GC-II and GC-III from both species have a highly conserved catalytic (GC) domain at the C terminus. (A) GC-Iβ has heme/NO-binding (HNOB) and heme/NO-binding-associated (HNOBA) domains, which are characteristic of NO-sensitive GCs. (B) GC-II has signal peptide (signal), ligand-binding (LB), transmembrane (TM), kinase homology (KH) and dimerization (DD) domains. (C) GC-III resembles the GC-II, but lacks the signal peptide, LB, TM and most of the KH domain. Amino acid residues, numbered from the N terminus to the C terminus, are indicated.

ESA, either singly or in combination with MLA, significantly increased hemolymph ecdysteroid levels at Day 28 and later time intervals, although the means never exceeded 30 pg µl^{-1} (Day 45; Fig. 4). There was no significant difference between the means of intact and MLA animals, except at Day 52 (Fig. 4).

Green morphs were divided into three treatment groups: intact (control), ESA and MLA. The experiment was initiated in February during the molting season. Hemolymph samples were taken at weekly intervals and ecdysteroid titers were determined. The 22 animals that were in intermolt at Day 0 did not molt for the duration of the experiment. MLA had no effect on hemolymph ecdysteroid levels, as there were no significant differences between the means of the intact and MLA animals at all time intervals, except at Day 63 (Fig. 5A). By contrast, ESA significantly increased hemolymph ecdysteroid levels at Day 21 and later time intervals, although the means never exceeded 53 pg µl^{-1} (Day 70; Fig. 5A). Eight animals were in premolt at the beginning of the experiment, as indicated by elevated ecdysteroids (72–196 pg µl^{-1}) at Day 0: two animals in the control group, three in the MLA group and three in the ESA group. MLA had no effect on molting of the premolt crabs; ecdysteroid levels in the premolt intact and MLA animals continued to increase and all five crabs molted within 4 weeks (Fig. 5, compare B and D). However, ESA delayed molting of premolt animals. The increase in hemolymph ecdysteroids was delayed in two animals, which molted at Day 40 and Day 90; in the third animal, ecdysteroid titer decreased and the animal did not molt during the experiment (Fig. 5C). Hemolymph ecdysteroid titers in molting animals peaked between 400 and 1000 pg µl^{-1} prior to ecdysis (Fig. 5B–D) (see also Styrishave et al., 2004b).

While conducting ESA experiments on the green morphs, we observed that ESA accelerated the transition from green to red pigmentation. This transition was documented by capturing digital images of the ventral surface of the thoracic segments of intact, MLA and ESA animals at 2-week intervals. Fig. 6A shows images of representative animals from each group. MLA resulted in the reddening of the arthrodial membranes of the basi-ischial joints, compared with those of the intact animals, which was noticeable by 4 weeks post-MLA (12 March 2010; Fig. 6A). There was also a slight reddening of the ventral cephalothorax 6 to 12 weeks post-MLA (Fig. 6A). ESA resulted in reddening of the basi-ischial

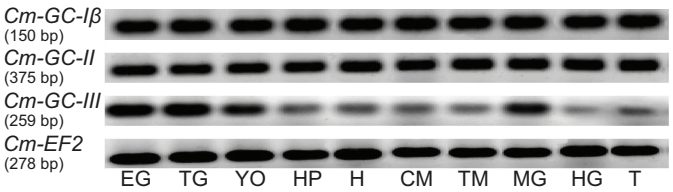

Fig. 2. Expression of guanylyl cyclases and elongation factor 2 (EF2) in *C. maenas* tissues. End-point PCR was used to determine the presence of *Cm-EF2*, *Cm-GC-Iβ*, *Cm-GC-II* and *Cm-GC-III* transcripts. EG, eyestalk ganglia; TG, thoracic ganglion; YO, Y-organ; HP, hepatopancreas; H, heart; CM, claw muscle; TM, thoracic muscle; MG, midgut; HG, hindgut; T, testis. Negative images of ethidium bromide-stained agarose gels are shown.

The Journal of Experimental Biology (2014) doi:10.1242/jeb.093385

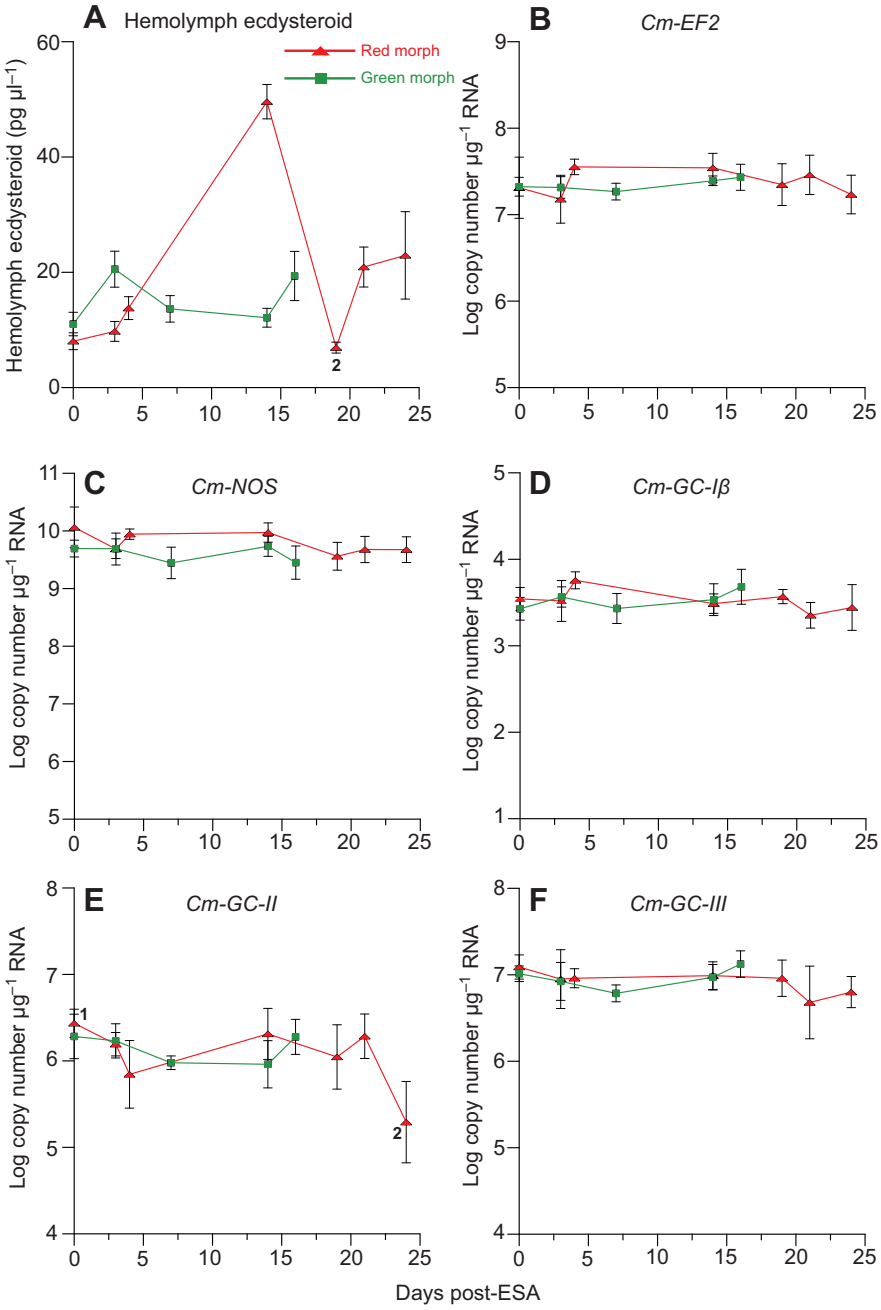

Fig. 3. Effects of eyestalk ablation (ESA) on hemolymph ecdysteroid, nitric oxide synthase (NOS) and guanylyl cyclase expression in red (triangles) and green (squares) morphs over 24 and 16 days, respectively. Animals were eyestalk-ablated at Day 0. YOs were harvested and hemolymph samples were taken at various intervals post-ESA. Ecdysteroid levels were quantified by ELISA. mRNA levels were quantified by qPCR. Data are presented as means ± 1 s.e.m. (red morph, *N*=7, 3, 6 and 3 at Days 0, 3, 14 and 24, respectively; green morph, *N*=13, 5, 5, 5 and 4 at Days 0, 3, 7, 14 and 16, respectively). Different letters (numbers) indicate green (red) morphs that are significantly different ($P<0.05$) from each other.

joints and ventral cephalothorax within 2 weeks and the red color became more intense at later time intervals (Fig. 6A). The images from all the animals were analyzed for changes in red, blue and green hues of the ventral exoskeleton. The results are presented as the ratio of green to red intensities, as green color was affected by treatment, while red and blue colors were relatively constant (data not shown). ESA significantly decreased the green to red color ratio (Fig. 6B). There was also a decrease in the green:red ratio in MLA animals, but the means were not significantly different from those of intact animals. We conclude that ESA caused a loss of green color, which revealed the red pigment present in the exoskeleton.

At the conclusion of the experiment, YOs were harvested and the expression of the three GCs and EF2 were quantified by qPCR (Fig. 7). In red morphs, long-term ESA decreased *Cm-EF2* mRNA level by approximately four orders of magnitude (13,100-fold) in the ESA group (9.34×10^{6} copy number per µg total RNA versus 1.23×10^{11} copy number per µg total RNA in intact) and approximately 21-fold in the ESA+MLA group (5.88×10^{9} copy number per µg total RNA versus 1.23×10^{11} copy number per µg total RNA). MLA decreased *Cm-EF2* mRNA level about 322-fold (3.81×10^{8} copy number per µg total RNA versus 1.23×10^{11} copy number per µg total RNA; Fig. 7A). The *Cm-GC-II* mRNA level was approximately 400-fold lower in the ESA animals than that in intact animals, and *Cm-GC-III* mRNA levels were about 36-fold and fourfold lower in ESA and MLA animals, respectively, than those in intact animals (Fig. 7A). By contrast, ESA and MLA had no significant effect on *Cm-GC-Iβ*, *Cm-GC-II*, *Cm-GC-III* or *Cm-EF2* mRNA levels in green morphs (Fig. 7B).

Effects of molting on *NOS*, *GC-Iβ*, *GC-II*, *GC-III* and *EF2* expression

As intermolt green and red morphs were refractory to molt induction by ESA and MLA, the expression of *Cm-NOS*, the three GCs, and

The Journal of Experimental Biology (2014) doi:10.1242/jeb.093385

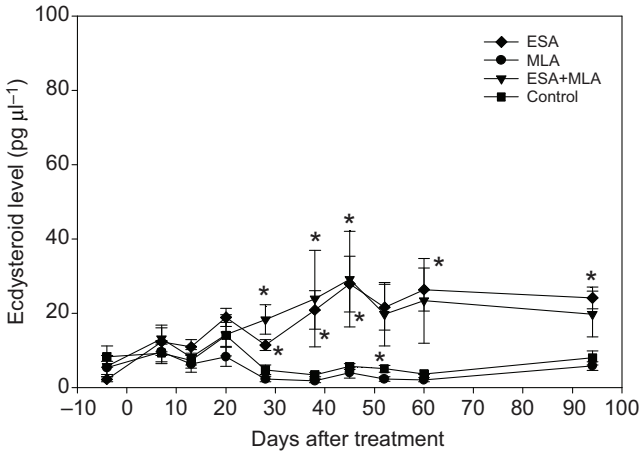

Fig. 4. Effects of ESA and multiple leg autotomy (MLA) on *C. maenas* hemolymph ecdysteroid levels in red morphs. Intermolt red morphs were divided into intact (control), ESA, MLA and ESA+MLA treatment groups, and hemolymph samples were taken at weekly intervals during the 3-month period. Data are presented as means ± 1 s.e.m. (*N*=3 for intact; *N*=4 for ESA; *N*=4 for MLA; *N*=4 for ESA+MLA). Asterisks indicate significant differences (**P*<0.05) between the means of ESA or ESA+MLA groups and the means of the intact or MLA groups.

Cm-EF2 were quantified in YOs from spontaneously molting green morphs. The hemolymph ecdysteroid levels increased at premolt, and decreased to low levels at postmolt (Fig. 8A). *Cm-GC-Iβ* mRNA increased approximately threefold at the premolt stage (Fig. 8B). *Cm-GC-III* mRNA level was 1.3-fold lower in premolt animals than in intermolt animals and 2.1-fold higher in postmolt animals than in intermolt animals (Fig. 8B). There were no significant differences in *Cm-NOS*, *Cm-GC-II* or *Cm-EF2* mRNA levels between the molt cycle stages (Fig. 8B).

Expression of *Cm-MIH* in the brain and thoracic ganglion

As ESA did not induce molting in intermolt animals, the brain and thoracic ganglion were investigated as secondary sources of MIH. Nested end-point PCR indicated that MIH was expressed in the brain and thoracic ganglion from intact intermolt green and red morphs (Fig. 9 and data not shown). The identity of the PCR product as Cm-MIH was verified by direct sequencing. cDNAs from claw and thoracic muscles were also tested under the same conditions as negative controls; nested PCR yielded no *Cm-MIH* product (Fig. 9). ESA had no significant effect on the expression of *Cm-MIH* or *Cm-EF2* in the brain and thoracic ganglion (Fig. 10).

DISCUSSION

Molting of red and green morphs

As an invasive species, *C. maenas* has altered coastal and estuarine communities (de Rivera et al., 2011; Grosholz, 2005; Grosholz and Ruiz, 1995; Grosholz et al., 2000; Kimbro et al., 2009). The expansion of this species has made it available to investigators outside of northern Europe and eastern North America. An understanding of molting and growth can inform decisions for predicting and possibly mitigating negative impacts as the species expands its range (Jamieson et al., 1998). However, any analysis must consider that populations vary genetically, which may contribute to physiological differences between geographical regions (Darling et al., 2008; Geller et al., 1997; Tepolt et al., 2009). Western North American populations differ from those in eastern North America and South Africa in habitat usage and size; compared with the other two regions, populations in central California have not colonized rocky shores, but they grow to a larger size (Grosholz and Ruiz, 1996). *Carcinus maenas* became established in Bodega Harbor in the mid-1990s and the population has lower genetic diversity than the native populations of northern Europe (Darling et al., 2008; Grosholz and Ruiz, 1995; Tepolt et al., 2009).

The intermolt interval in *C. maenas* increases as adults mature from the green to red color morph. Juveniles occur in the green phenotype; they molt frequently throughout the year and reach adulthood by 25–30 mm CW (Bückmann and Adelung, 1964; Crothers, 1967; Saïdi et al., 1994; Styrishave et al., 2004a). As the green morphs molt to larger sizes, they transition to red morphs during a prolonged intermolt period (McGaw et al., 1992). Older red morphs stop molting entirely and enter a blocked or terminal anecdysis state (Baghdassarian et al., 1996; Carlisle, 1957; Crothers, 1967; Lachaise et al., 1988; Saïdi et al., 1994; Styrishave et al., 2004a; Styrishave et al., 2004b; Webster, 1986). Large males (CW >70 mm) never show signs of molting (e.g. limb regeneration) and ecdysteroid titers never exceed 70 pg µl^{-1} (Carlisle, 1957; Webster, 1986). Although green morphs tend to be smaller than red morphs, there is a large overlap in size distribution (McGaw et al., 1992; Reid et al., 1997; Styrishave et al., 2004b). When red morphs molt they molt back to the green phenotype [S.N., D.L.M. and E.S.C., unpublished; also inferred from the data presented in McGaw et al. (McGaw et al., 1992)], which may explain the occurrence of green morphs in the larger size classes (CW >60 mm).

Crabs from Bodega Harbor provided an opportunity to determine the effects of two commonly used molt-induction techniques on a recently introduced and genetically distinct population. Unlike northern Europe, older individuals are rarely captured in the intertidal region of Bodega Harbor. The animals used in this study were an estimated 1 to 2 years in age. They were sexually mature, but were not blocked or in terminal anecdysis, based on the absence of epibionts usually found on older individuals and our observations of molting in captive animals. Thus, we were able to investigate potential differences between color morphs in response to ESA and MLA. We hypothesized that green morphs would be more responsive to ESA or MLA than red morphs, as green morphs invest more energy in growth and red morphs invest more energy into reproduction (Reid et al., 1997; Styrishave et al., 2004a).

Juvenile (CW <25 mm) and adult (CW >25 mm) *C. maenas* differ in response to molt induction methods. In juveniles, 20-hydroxyecdysone (20E) injections, ESA and MLA stimulate molting (Adelung, 1971; Bazin, 1977a; Bazin, 1977b; Bückmann and Adelung, 1964; Spindler et al., 1974). The published data on adults from north Atlantic populations are not consistent. In intermolt animals (color morph and sizes were not given), neither ESA nor 20E injections induced molting (Buchholz and Adelung, 1979; Carlisle, 1954; Saïdi et al., 1994; Skinner and Graham, 1972). However, Carlisle (Carlisle, 1957) reported that ESA induced animals in terminal anecdysis to molt, and Skinner and Graham (Skinner and Graham, 1972) reported that MLA accelerated molting in adults. From our observations, both color morphs from the Bodega Harbor population were refractory to MLA or ESA, either separately or in combination, even after 3 months (Fig. 4, Fig. 5A). The discrepancies between our results and previously published work may be due to genetic differences between the Bodega Harbor population and the populations in eastern North America and northern Europe.

An unexpected result was the acceleration in the transition from the green to the red morph by ESA (Fig. 6). Color change in crustaceans has long been known to be dependent on eyestalk

The Journal of Experimental Biology (2014) doi:10.1242/jeb.093385

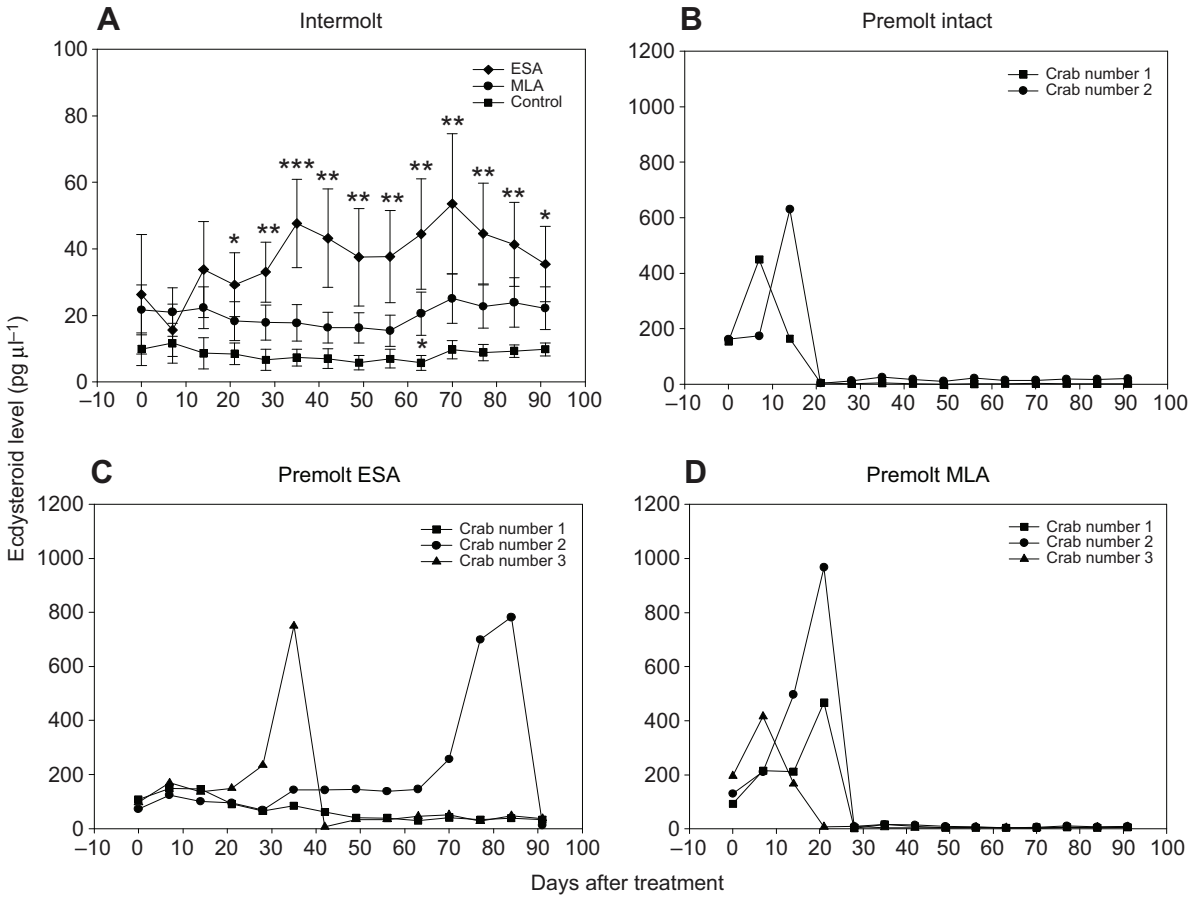

Fig. 5. Effects of ESA and MLA on *C. maenas* hemolymph ecdysteroid levels in green morphs. Green morphs were divided into intact, ESA and MLA treatment groups, and hemolymph samples were taken at weekly intervals during the 3-month period. (A) Animals that were in intermolt at Day 0. Data are presented as means ± 1 s.e.m. (intact, *N*=10; ESA, *N*=9; MLA, *N*=18). Animals that were in early premolt at Day 0 are graphed separately for individual crabs: (B) intact animals; (C) ESA animals; (D) MLA animals. Asterisks indicate significant differences between the means of the ESA or MLA groups and the intact control group (*P<0.05; **P<0.01; ***P<0.001).

factors (Pouchet, 1872; Shibley, 1968). The body of most crabs blanches after ESA as a result of concentration of pigment in chromatophores (Shibley, 1968). Injection of eyestalk extracts into the animal temporarily reverses the condition (Abramowitz, 1937; Carlson, 1936; Kleinholz, 1961; Shibley, 1968; reviewed by Fingerman, 1965). Also, ESA can abolish daily rhythmic color changes in the fiddler crab, *Uca*, and the crayfish *Astacus* (reviewed by Brown, 1961). Lenel and Veillet (Lenel and Veillet, 1951) reported changes in color after removing the eyestalks of *C. maenas*. The pigmentary layer of the new cuticle was affected first and then the epidermal chromatophores (Lenel and Veillet, 1951; reviewed by Goodwin, 1960). This change in color was not due to increased accumulation of the carotenoid astaxanthin, but rather to the dissociation of the brown and green astaxanthin–protein complex (Lenel and Veillet, 1951). Our results were consistent with those of Lenel and Veillet (Lenel and Veillet, 1951). The ESA treatment group showed a strong decline in the green:red ratio from the first 2 weeks until the end of the experiment (Fig. 6). There was no change in red color intensity, which presumably measured the amount of astaxanthin, in ESA and MLA animals. The color change was not strictly linked to molting, as green morphs remained in intermolt (indicated by low hemolymph ecdysteroid titers and presence of the membranous layer at the end of the experiment) and did not molt. The green:red ratio of MLA animals showed a decreasing trend, but it was not significantly different from intact animals (Fig. 6). This suggests that MLA can alter the synthesis and/or release of eyestalk neuroendocrine factor regulating green to red transformation. The identity of this factor and its mode of action require further investigation.

Effects of molting on gene expression

The effects of ESA and MLA on gene expression differed between the *C. maenas* color morphs, but the differences were not apparent until 90 days after treatment. There was little or no effect of ESA on *Cm-NOS*, *Cm-EF2* or *Cm-GC* expression in the YO from green and red morphs in the intermediate-interval experiment (Fig. 3). At 90 days, *Cm-EF2* and *Cm-GC* mRNA levels in green morphs were not affected by ESA and MLA (Fig. 7B). Prolonged ESA appeared to have deleterious effects on red morphs, as there were large decreases in *Cm-EF2*, *Cm-GC-II* and *Cm-GC-III* mRNA levels in ESA animals (Fig. 7A). *EF2* is a constitutively expressed housekeeping gene necessary for translation. The changes in *Cm-GC-II* and *Cm-GC-III* expression in the 90-day ESA red morphs were one to four orders of magnitude greater than those in spontaneously molting green morphs (compare Fig. 7A with Fig. 8B). The reduced expression of *Cm-GC-II* and *Cm-GC-III* may inhibit neuropeptide signaling in the YO. Prolonged ESA can disrupt molting processes in *C. maenas*. In a group of red morphs that had been eyestalk ablated for approximately 8 months, a few animals molted back to green morphs but failed to harden the new exoskeleton and

The Journal of Experimental Biology (2014) doi:10.1242/jeb.093385

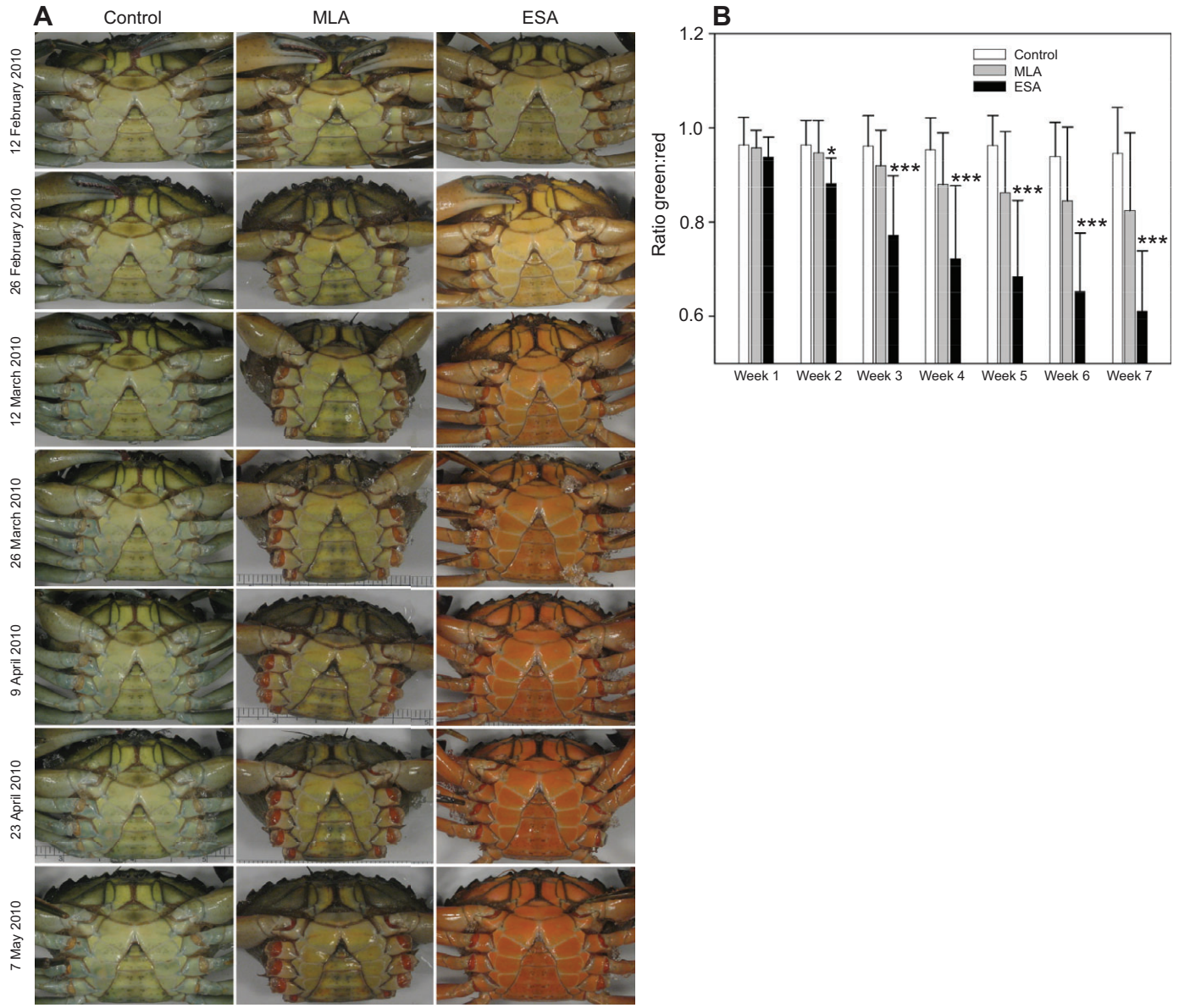

Fig. 6. Effects of ESA and MLA on *C. maenas* green morph ventral pigmentation. (A) Representative images of individual crabs from intact, ESA and MLA treatment groups captured at 2-week intervals for 12 weeks (see Materials and methods). Approximate width of each panel is equivalent to 5 cm. (B) Ratio of green to red color intensities of the left thoracic sternum of intact (*N*=10), MLA (*N*=20) and ESA (*N*=10) animals (means ± 1 s.d.; see Materials and methods). Asterisks indicate significant differences between the control and ESA crabs (*P<0.05; ***P<0.001). There were no significant differences between the intact and MLA animals.

eventually died (S.N. and D.L.M., unpublished). This indicates that eyestalk neurosecretory factors, either directly or indirectly, are required for synthesis and calcification of the exoskeleton during the postmolt period. Taken together, the data suggest that the green morphs tolerate prolonged ESA treatment better than the red morphs. This is consistent with reports that green morphs are more tolerant of extremes in temperature, salinity and oxygen levels than red morphs (reviewed by Styrishave et al., 2004a). The data also indicate that the red morphs used in the study were capable of molting and that they were not in terminal anecdysis.

Gene expression in YOs from *C. maenas* and *G. lateralis* differ in response to ESA. ESA increases *Gl-NOS*, *Gl-GC-Iβ* and *Gl-GC-III* expression in *G. lateralis* (Lee et al., 2007a; McDonald et al., 2011). By contrast, ESA had little or no effect on *Cm-NOS*, *Cm-GC-Iβ* or *Cm-GC-III* expression in *C. maenas* nor was there any correlation with hemolymph ecdysteroid levels (Fig. 3). In the land crab, *Gl-NOS* and *Gl-GC-Iβ* transcript copy numbers are correlated with hemolymph ecdysteroid levels (Lee et al., 2007a; McDonald et al., 2011), indicating that expression of these genes is associated with YO activation. The differences in the effect of ESA on *NOS* and *GC-Iβ* gene expression in the two species can be attributed to whether ESA induces molting. Both *C. maenas* color morphs were resistant to ESA (Figs 4, 5), while *G. lateralis* enter premolt immediately and molt by 3 weeks post-ESA (Covi et al., 2010).

Effects of ESA

Even though ESA does not trigger molting in the Bodega Harbor population, it causes small, transient increases in hemolymph ecdysteroid concentration during the first 2 weeks post-ESA (Fig. 3A). Interestingly, there were small, sustained increases in

The Journal of Experimental Biology (2014) doi:10.1242/jeb.093385

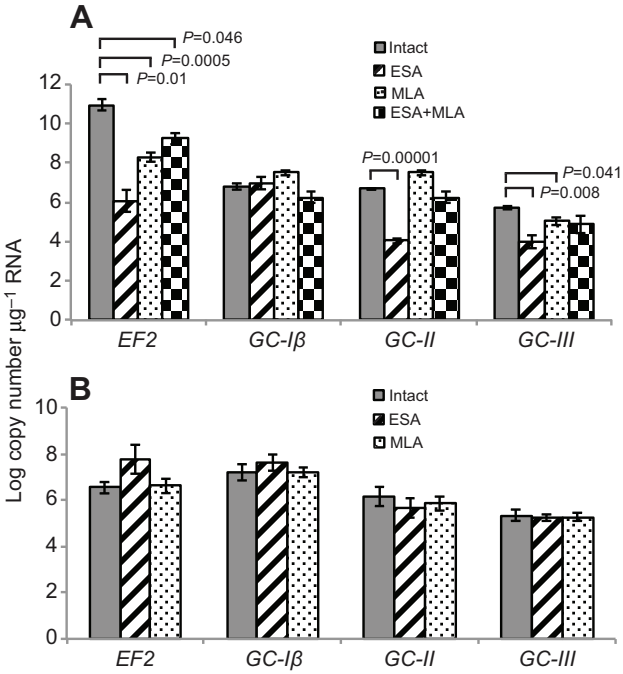

Fig. 7. Effects of long-term ESA and MLA on YO expression of guanylyl cyclases (*Cm-GC-Iβ*, *Cm-GC-II* and *Cm-GC-III*) and *Cm-EF2* in red and green morphs. (A) Red morphs were divided into four treatment groups: intact (control), ESA, MLA and ESA+MLA. (B) Green morphs were divided into three treatment groups: intact, ESA, and MLA. YOs were harvested 90 days post-treatment and transcripts were quantified by real-time PCR (see Materials and methods). Data are presented as means ± 1 s.e.m. (red morph treatment groups: intact, *N*=3; ESA, *N*=5; MLA, *N*=4; ESA+MLA, *N*=5; green morph treatment groups: intact, *N*=8; ESA, *N*=8; MLA, *N*=17). Means that were significantly different from each other are indicated by a bracket with the corresponding *P*-value.

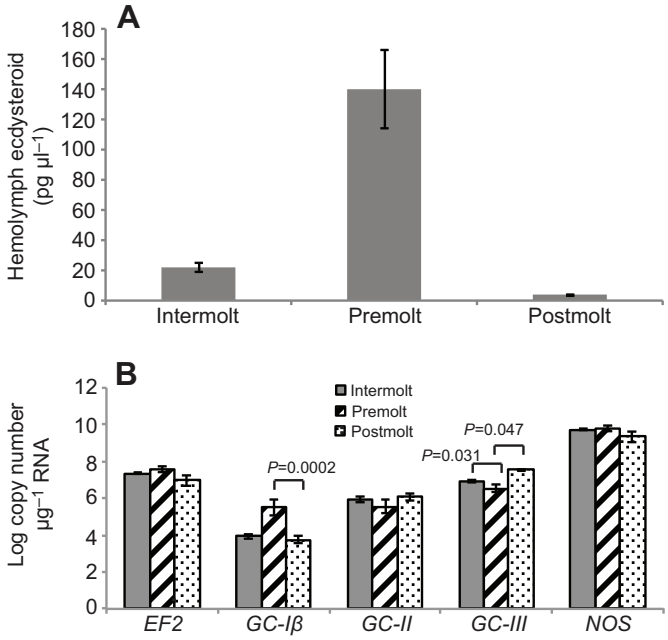

Fig. 8. Effects of molting on (A) hemolymph ecdysteroid levels and (B) expression of guanylyl cyclases and *Cm-NOS* in green morph *C. maenas* YOs. Hemolymph and YOs were collected from spontaneously molting green morphs grouped into intermolt, premolt and postmolt stages (see Materials and methods). Data are presented as means ± 1 s.e.m. (intermolt *N*=62, premolt *N*=18, postmolt *N*=4). In A, all means are significantly different (*P*<0.05) from each other. In B, means that are significantly different from each other are indicated by a bracket with the corresponding *P*-value.

ecdysteroid titers of approximately fourfold to fivefold in eyestalk-ablated crabs, beginning 21 days post-ESA in green morphs and 28 days post-ESA in red morphs (Fig. 4, Fig. 5A). Green morphs tended to have higher ecdysteroid titers than red morphs, although the levels were not significantly different. This is consistent with the findings of Styrishave et al. (Styrishave et al., 2004b), who found no difference in hemolymph 20E titers in intermolt red and green morphs, although larger animals had lower levels than smaller animals. The increased ecdysteroid titer was sustained until the termination of the experiment at Day 90, and never exceeded 60 pg µl^{-1}, indicating that the animals did not progress through premolt (Fig. 4, Fig. 5A). This is in contrast to molting animals, in which hemolymph ecdysteroid concentration increased, reaching a peak exceeding 400 pg µl^{-1} in late premolt (Fig. 5B–D). A surprising result was the effect of ESA on premolt animals. Rather than stimulating molting, ESA delayed molting in two animals and a third animal did not molt by 90 days post-ESA (Fig. 5C). These data suggest that the YO of intermolt *C. maenas* cannot be activated by acute withdrawal of MIH produced by the XO/SG complex. Moreover, once the YO is activated in early premolt, it can be inhibited by ESA.

Expression of *Cm-MIH* in the brain and thoracic ganglion

As ESA failed to induce molting in intermolt *C. maenas* and delays molting in premolt *C. maenas*, we considered that there are extra-eyestalk MIH neurosecretory cells in the nervous system. These cells may produce and secrete sufficient amounts of MIH to prevent molting in intermolt animals. They would also delay molting in early premolt animals, as activated YOs are sensitive to MIH until they transition to the committed state in mid-premolt (Chung and Webster, 2003; Chang and Mykles, 2011). The brain (supraesophageal ganglion) and thoracic ganglion contain numerous neurosecretory cells (Bliss et al., 1954; Christie, 2011; reviewed by Cooke and Sullivan, 1982). Although most of the axons that terminate in the sinus gland originate from cell bodies in the X-organ, the sinus gland receives input from neurons in the brain, circumesophageal connectives and thoracic ganglion; these neurons may be secretory or non-secretory (Andrew et al., 1978; Bliss et al., 1954; Bliss and Welsh, 1952; Cooke and Sullivan, 1982; Jaros,

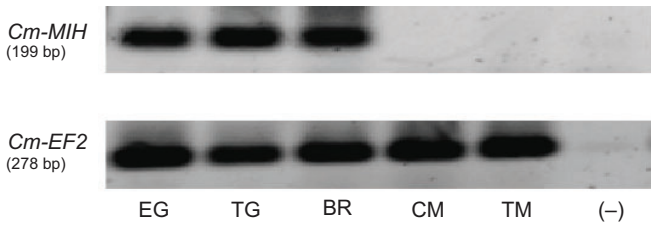

Fig. 9. Expression of *Cm-MIH* and *Cm-EF2* in eyestalk ganglia (EG), thoracic ganglion (TG), brain (BR), claw muscle (CM) and thoracic muscle (TM) from intermolt green morph *C. maenas*. Nested end-point PCR was used to detect *Cm-MIH* transcript in cDNA from brain, thoracic ganglion and muscle (35 cycles for each round). A non-nested PCR was used to detect *Cm-MIH* in eyestalk ganglia (35 cycles with the inner primer pair) and *Cm-EF2* in cDNA from brain, thoracic ganglion and muscle (35 cycles; see Materials and methods). Negative images of ethidium bromide-stained agarose gels are shown.

The Journal of Experimental Biology (2014) doi:10.1242/jeb.093385

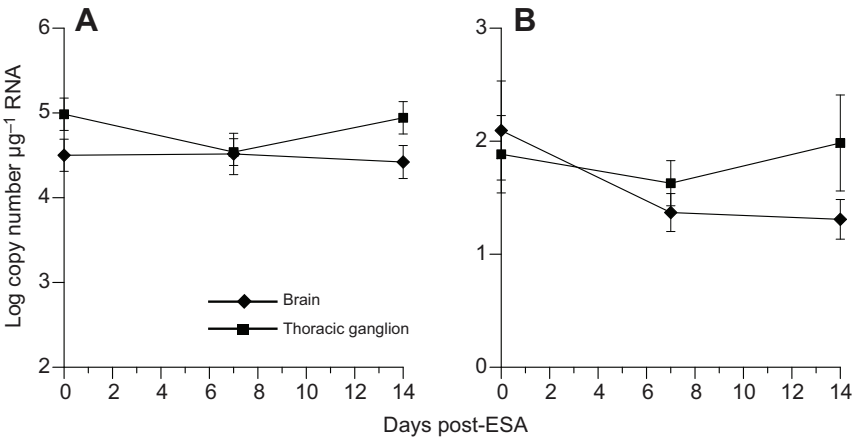

Fig. 10. Effects of ESA on expression of (A) *Cm-EF2* and (B) *Cm-MIH* in the brain (diamonds) and thoracic ganglion (squares) of both color morphs of *C. maenas*. Transcript levels were quantified by qPCR. Data are presented as means ± 1 s.e.m. (brain, *N*=18 at Day 0, *N*=13 at Day 7 and *N*=15 at Day 14; thoracic ganglion, *N*=25 at Day 0, *N*=15 at Day 7 and *N*=20 at Day 14).

1978). The only physiological evidence that the brain and circumesophageal connectives have molt-inhibitory activity is a brief report by Stephens (Stephens, 1951). Implantation of brain and circumesophageal connectives into crayfish in which eyestalks or sinus glands were removed reduced molting frequency from 42% in a control group to 5% over a 2.5-week period (Stephens, 1951). RT-PCR indicates that the *Metapenaeus ensis* (Me) MIH-A isoform is expressed only in eyestalk, but the Me-MIH-B isoform is expressed in eyestalk, brain, thoracic ganglion, and ventral nerve cord (Tiu and Chan, 2007). In the swimming crab *Portunus trituberculatus*, MIH is expressed in the eyestalk ganglia, brain, thoracic ganglion and gonadal tissues (Zhu et al., 2011). In *Cancer pagurus*, MIH is expressed in the eyestalk, optic nerve, ventral nerve cord and thoracic/abdominal ganglia (Lu et al., 2001). The results of the nested PCR analysis (Fig. 9) clearly showed the presence of a PCR product of the expected size of MIH (199 bp) in the brain and thoracic ganglion. The identity of the PCR product to Cm-MIH was confirmed by direct sequencing. However, we considered the possibility of cross-contamination of PCR reactions of the thoracic ganglion and brain preparations with MIH mRNA or cDNA. Although we cannot completely rule out this possibility, this is less likely, as the muscle cDNAs, as well as the water control, did not yield the MIH PCR product (Fig. 9). A recent study of *Portunus pelagicus* showed the MIH peptide localized in neurons in the XO/SG complex, brain, esophageal ganglion and thoracic ganglion, indicating that the mRNA in extra-eyestalk nervous tissues is translated into protein (Stewart et al., 2013). MIH immunoreactivity is restricted to a small number of neurons in the brain and thoracic ganglion (Stewart et al., 2013). This is consistent with the low *Cm-MIH* mRNA levels in the brain and thoracic ganglion (Fig. 10B), which are several orders of magnitude lower than that in the eyestalk ganglia (N. L. Pitts and D.L.M., unpublished data). It remains to be determined whether secondary sources are sufficient to inhibit molting in eyestalk-ablated *C. maenas*, although the implantation experiments on crayfish show that brain and circumesophageal connectives produce sufficient amounts of an MIH-like factor (Stephens, 1951).

Neuropeptide regulation of the YO in adult *C. maenas* has been studied in naturally molting animals collected from European populations over the May to November molting season (Baghdassarian et al., 1996; Chung and Webster, 2003; Lachaise et al., 1988; Saïdi et al., 1994; Toullec and Dauphin-Villemant, 1994). In *C. maenas* and crayfish (*P. clarkii*), the YO becomes less sensitive to MIH and CHH during mid and late premolt, which coincides with the commitment of the animal to proceed to ecdysis (Chung and Webster, 2003; Nakatsuji and Sonobe, 2004; Nakatsuji et al., 2006). As there is no decrease in high-affinity membrane receptors (Chung and Webster, 2003), the reduced sensitivity to MIH is downstream from ligand-receptor binding. A hypothetical model of the MIH signaling pathway is arranged into cAMP- and cGMP-dependent phases. The 'triggering' phase produces a rapid, transient increase in cAMP, influx of Ca^{2+}, and binding of Ca^{2+} to CaM; the 'summation' phase follows when Ca^{2+}/CaM activates NOS, which, in turn, activates GC-I and produces a large sustained increase in cGMP (reviewed by Chang and Mykles, 2011; Covi et al., 2012; Webster et al., 2012). An increase in phosphodiesterase (PDE) activity contributes to reduced MIH sensitivity by lowering cyclic nucleotide levels, as IBMX, a PDE inhibitor, increases the sensitivity of the YO to MIH (Nakatsuji et al., 2006). Moreover, the MIH- and CHH-dependent increases in cGMP concentrations in the *C. maenas* YO are the lowest at mid and late premolt (stages D_1 and $D_{2–3}$) and early postmolt (stage A) (Chung and Webster, 2003). However, the magnitude in the increase in PDE activity cannot account entirely for the magnitude in the decrease in MIH response, suggesting that key MIH signaling components, such as NOS and GC, may be downregulated during premolt (Chang and Mykles, 2011). The expression of *Cm-GC-III*, which is an NO-insensitive GC, is consistent with the hypothesis; its mRNA levels decreased during premolt (Fig. 8B). The Gl-GC-III is a constitutively active soluble GC and may act synergistically with Gl-GC-I to increase intracellular cGMP levels (Lee et al., 2007a). Although the increase in *Cm-GC-Iβ* expression during premolt (Fig. 8B) is not consistent with the hypothesis, it resembles the increase in *Gl-GC-Iβ* mRNA when the *G. lateralis* YO is activated by ESA (Lee et al., 2007a). The ecdysteroid titers and the structure of the integument indicated that 13 of the 18 premolt animals were in early premolt (Stage D_0; compare ecdysteroid titers in Fig. 8A with those in Fig. 5B–D). The *C. maenas* YO is the least sensitive to MIH and CHH at stages D_1, $D_{2–3}$ and A–B (Chung and Webster, 2003). Thus, the matter remains unresolved until the expression of MIH signaling components is quantified in YOs from animals at late premolt stages (D_1 and $D_{2–3}$).

Conclusions

Both color morphs of adult *C. maenas* from a western North America population were refractory to molt induction by ESA and MLA. ESA accelerated a shift from the green to red coloration, indicating that an eyestalk neuroendocrine factor is involved. MIH does not appear to be the factor, as the transition occurred while the animals remained in intermolt. The change in color was due to a decrease in green color, which unmasked the red pigment astaxanthin and made it more visible. ESA did not activate the YO, as ESA had little or no effect on hemolymph ecdysteroid titers and

on the expression of the three guanylyl cyclases and NOS for up to 24 days after treatment. Prolonged ESA appeared to have deleterious effects on molting processes in red morphs, as there were large decreases in YO gene expression and disruption of exoskeleton synthesis and calcification in postmolt animals. This is consistent with the XO/SG complex as an essential neurosecretory center controlling a wide diversity of physiological functions. The expression of *Cm-GC-Iβ* and *Cm-GC-III* was responsive to molting, but the changes in the expression of the two genes were in opposite directions. The MIH transcript is present in the brain and thoracic ganglion of intermolt crabs. MIH expression was not affected by ESA, indicating that the MIH gene was not regulated transcriptionally by the loss of the eyestalks. Taken together, the data suggest that the brain and thoracic ganglion serve as secondary sources of MIH. The data also suggest that the MIH produced from these sources is sufficient to prevent activation of the YO, as well as inhibit the activated YO in early premolt green morphs, when the primary source of MIH is removed by ESA.

MATERIALS AND METHODS

Animals and experimental treatments

Adult male green crabs, *C. maenas* (CW=47–89 mm), were collected from the harbor at Bodega Bay, California. The animals were 1 to 2 years in age and were capable of molting, which was based on observations of animals in captivity. They were maintained under flow-through conditions at ~13°C in the facilities of the Bodega Marine Laboratory and fed squid twice per week. Some crabs were shipped to Colorado. In Colorado, animals were kept in aerated water with a salinity of 30 ppt (Instant Ocean, Aquarium Systems, Mentor, OH, USA) at 20°C on a 12 h:12 h dark:light cycle. They were fed cooked chicken liver once a week and water was changed after feeding. For ESA and MLA, we used the same procedures as those described for *G. lateralis* (Lee et al., 2007a; Skinner and Graham, 1972). Green morphs undergoing natural molts were collected in February to April 2010 and 2011.

Intermediate-interval experiments determined the effects of ESA in green and red morphs for up to 24 days. YOs were harvested from intact (Day 0) animals and from ESA animals at various intervals post-ESA. Hemolymph samples (100 µl) were taken at the time of harvest and combined with 300 µl methanol for enzyme-linked immunosorbent assay (ELISA) analysis modified from Kingan (Kingan, 1989) and Tamone et al. (Tamone et al., 2007) (see Appendix).

Long-term experiments determined the effects of ESA and MLA after ~3 months in green and red morphs. Green morph animals from the winter molting season were divided into three treatment groups: intact control (*N*=10), ESA (*N*=9) and MLA (*N*=18). All eight walking legs were autotomized in the MLA group. Digital images of the ventral area of each crab were acquired every 2 weeks at the same settings. Images were analyzed with Photoshop CS software using the 'Info' tab to quantify the intensities of red, green and blue from the center of the first thoracic sternum on the crab's left side. Results were analyzed by one-way ANOVA using SigmaStat version 3.00 (SYSTAT Software, San Jose, CA, USA). Red morph animals from the late spring season were divided into four treatment groups: intact control (*N*=3), ESA (*N*=4), MLA (*N*=4) and ESA+MLA (*N*=4). Every week, hemolymph samples (50 µl) were combined with 350 µl methanol for ELISA (see Appendix). After ~90 days, the YOs were harvested, frozen in liquid nitrogen and stored at −80°C.

RNA isolation and mRNA analysis

The RNA isolation protocol is described in Covi et al. (Covi et al., 2010). Animals were anesthetized with ice for 5 min prior to dissection of the YO and other tissues. Hemolymph samples (100 µl) were combined with 300 µl methanol for quantification of ecdysteroids by radioimmunoassay (Medler et al., 2005) or ELISA (see Appendix). Tissues were frozen in liquid nitrogen and stored at −80°C. Total RNA was isolated using TRIzol reagent (Invitrogen, Carlsbad, CA, USA) using the manufacturer's protocol. Total RNA was treated with DNase I for 30 min, extracted with phenol:chloroform:isoamyl alcohol (25:24:1), precipitated with 1 volume of isopropanol, and dissolved in 30 µl nuclease-free water (Integrated DNA Technology, Coralville, IA, USA). RNA concentration was determined by absorbance at 260 nm using a NanoDrop ND-1000 Spectrophotometer (Thermo Fisher Scientific, Waltham, MA, USA). cDNA was synthesized in reactions (20 µl) containing 1 µg RNA, 4 µl Transcriptor RT reaction buffer (Roche Applied Science, Indianapolis, IN, USA), 0.5 µl Ribolock RNase Inhibitor (40 u μl^{-1}; Fermentas, Glen Burnie, MD, USA), 0.5 µl reverse transcriptase (Roche), 2.0 µl dNTP (10 mmol l^{-1}) and 5 µl nuclease-free water. Complementary RNA was removed with RNase H (New England Biolabs, Ipswich, MA, USA).

The tissue distribution of *C. maenas* GCs (*Cm-GC-Iβ*, *Cm-GC-II* and *Cm-GC-III*), *Cm-MIH* (GenBank accession no. X75995) (Klein et al., 1993) and *Cm-EF2* (GU808334) (McDonald et al., 2011) was determined by end-point PCR. Reactions contained 1 µl template cDNA and 5 pmol each of the appropriate expression primers (Table 2) in Master Mix 2 (Thermo Fisher Scientific). Denaturation at 94°C for 3 min was followed by 30 or 35 cycles of 94°C for 30 s, lowest annealing temperature of a primer pair (Table 2) for 30 s, and 72°C for 30 s. Final extension was for 7 min at 72°C. After PCR was terminated, products were separated on a 1% agarose gel containing 40 mmol l^{-1} Tris acetate and 2 mmol l^{-1} EDTA (pH 8.5). The gels were stained with ethidium bromide and visualized with a UV light source. PCR products were purified using Qiaex II Gel Extraction kit (Qiagen). *Cm-EF2* is constitutively expressed and served as the control for RNA isolation and cDNA synthesis.

A Light Cycler Fast Start DNA Master PLUS SYBR Green I reaction mix and a Light Cycler 480 thermal cycler (Roche Applied Science) were used for quantitative analysis of *Cm-GC-Iβ*, *Cm-GC-II*, *Cm-GC-III* and *Cm-NOS* (GenBank accession no. GQ862349), *Cm-MIH* and *Cm-EF2*.

Table 2. Primers used for quantifying *Cm-MIH*, *Cm-NOS*, *Cm-EF2*, *Cm-GC-Iβ*, *Cm-GC-II* and *Cm-GC-III* mRNA levels using qPCR

Primer	Sequence (5′ to 3′)	Product size (bp)	Annealing temperature (°C)
Cm-NOS F4	GTGTGGAAGAAGAACAAGGACG	158	56
Cm-NOS R1	TCTGTGGCATAGAGGATGGTGG		
Cm-EF2 F1	CCATCAAGAGCTCCGACAATGAGCG	278	61
Cm-EF2 R1	CATTTCGGCACGGTACTTCTGAGCG		
Cm-GC-Iβ F8	CAAGATGATGGGTTCGCCTTCACCTACC	149	61
Cm-GC-Iβ R7	CTCTCTCTGGTCGTGTCTCTGCCTC		
Cm-GC-II F3	CGGTGGGTGGTGAAGATCAG	375	60
Cm-GC-II R3	CTCCGCCCAGCACTCCGTC		
Cm-GC-III F7	CCTCCTCACACAAAGACTCCAACGC	259	60
Cm-GC-III R8	GTGTGCCGTTACTAGACGAGAAATACGC		
Cm-MIH F1	TATCGGTGGTGGTTCTGG	281	56
Cm-MIH R1	AGCCCCAAGAATGCCAACC		
Cm-MIH F2	CGGCGAGAGTTATCAACG	199	54
Cm-MIH R2	TCTCTCAGCTCTTCGGACC		

Cm, *C. maenas*; EF2, elongation factor 2; F, forward; MIH, molt-inhibiting hormone; NOS, nitric oxide synthase; R, reverse; GC, guanylyl cyclase.

The Journal of Experimental Biology (2014) doi:10.1242/jeb.093385

qPCR reactions contained 1 µl cDNA, 5 µl 2× SYBR Green I Master Mix, 0.5 µl (10 mmol l^{-1}) each of forward and reverse gene-specific primers (Table 2) and 3 µl of PCR-grade water. The PCR conditions were an initial 95°C for 5 min, followed by 45 cycles of 95°C for 5 s (denaturation), 62°C for 5 s (annealing) and 72°C for 20 s (extension). Melting temperature analysis of the PCR products and the concentrations of the PCR transcripts used Roche version 1.2 of the Light Cycler 480 software. Standard curves were prepared by serial dilutions of purified PCR products (10^{-8} to 10^{-16} ng μl^{-1}).

Statistical analysis was performed using JMP 5.1.2 software (SAS institute, Inc., Cary, NC, USA). All qPCR data were log transformed to reduce the variance of the mean. Means for transcript abundance were compared using an ANOVA for days post-ESA versus log copy number. An ANOVA was also used to compare the means of naturally molting animals in various molting stages versus log copy numbers. A paired *t*-test was used to compare the means for transcript abundance between red and green morphs and hemolymph ecdysteroid concentration versus log copy number. A Grubb's test (extreme studentized deviate) was used to detect outliers. The level of significance for the all of the data analyses was set at α=0.05.

APPENDIX

Ecdysteroid ELISA

Plates (96-well, Costar 3366, Corning, NY, USA) were coated with AffiniPure goat anti-rabbit IgG Fc fragment antiserum (Jackson ImmunoResearch Labs 111-005-008, West Grove, PA, USA; 0.5 µg in 90 µl per well) in phosphate-buffered saline (PBS; 10 mmol l^{-1} sodium phosphate, 0.15 mol l^{-1} NaCl, pH 7.5) for 2 h at 23°C. The wells were aspirated and then incubated with assay buffer (AB; 25 mmol l^{-1} sodium phosphate, pH 7.5; 150 mmol l^{-1} NaCl; and 1 mmol l^{-1} EDTA disodium dehydrate; 300 µl per well) containing 0.1% bovine serum albumin (BSA, Fraction V; Sigma-Aldrich, St Louis, MO, USA) for 2 h at 23°C. The wells were washed three times with PBS containing 0.05% Tween 20 (PBS-T; Sigma-Aldrich). All samples were run in duplicate. Nonspecific binding was determined by loading two wells with AB containing 0.1% BSA (100 µl per well). Standards ranged from 0 to 120 pg 20E (Sigma-Aldrich) in AB containing 0.1% BSA (50 µl per well). Hemolymph samples in methanol were centrifuged for 10 min at 20,000 ***g*** at 4°C to remove precipitated protein. Supernatants (10 µl) were dried under vacuum in a Speed Vac centrifuge (Savant, West Palm Beach, FL, USA) and dissolved in 150 µl AB containing 0.1% BSA. Samples (50 µl), in duplicate, were loaded into each well. An internal standard consisting of lobster (*Homarus americanus*) hemolymph was included to assess inter-assay variation. 20E conjugated to horseradish peroxidase (HRP) reagent (1:64,000 dilution in AB with 0.1% BSA; 50 µl) was added to all wells and incubated on an orbital shaker for 5 min at 23°C. A rabbit anti-ecdysteroid primary antibody (50 µl; 1:100,000 dilution in AB with 0.1% BSA) was added to all wells, except for the first two wells containing AB plus 0.1% BSA. The 20E/HRP conjugate and 20E antibody were obtained from Dr Timothy Kingan (timkingan@gmail.com). The antibody preferentially binds to 20E (Kingan, 1989). The plates were sealed with Parafilm and incubated overnight at 4°C. Equal volumes of Solutions A and B of a tetramethylbenzidine-peroxidase kit (KPL, Gaithersburg, MD, USA) were combined at room temperature and 100 µl was added to each well. The plates were incubated for 15 min at 23°C in the dark. The reaction was stopped by the addition of 100 µl of 1 mol l^{-1} phosphoric acid and read with a Genios plate reader (Tecan, San Jose, CA, USA) at 450 nm. The data were archived with Magellan 6 (Tecan) and analyzed with Microplate Manager software (Bio-Rad Laboratories, Hercules, CA, USA).

Cloning of *C. maenas* GCs

RT-PCR and RACE were used to clone partial cDNAs encoding *Cm-GCIβ*, *Cm-GCII* and *Cm-GCIII*. Initial partial cDNA sequences for *Cm-GCIβ*, *Cm-GCII* and *Cm-GCIII* were obtained by designing nested degenerate primers to highly conserved sequences in the catalytic domain of *G. lateralis* GCs (Lee et al., 2007b). Mixed tissue cDNA from YO, claw muscle and thoracic ganglion was used for the initial PCR (RNA isolation and cDNA synthesis are described below). The PCR conditions were an initial denaturation at 96°C for 4 min followed by 35 cycles of denaturation for 30 s at 96°C, annealing for 30 s at the appropriate melting temperature for the specific primer set (supplementary material Table S1), and extension for 30–90 s at 72°C. Extension time varied with expected product size allowing 30 s for every 500 bp. PCR consisted of 1 µl cDNA template, 0.5 µl each forward and reverse primers (Table 1), 5 µl GoTaq Green Master Mix (Promega, Madison, WI, USA) and 3 µl sterile deionized water (Integrated DNA Technology). Reactions were performed using a Veriti 96 Well Thermal Cycler (Applied Biosystems, Foster City, CA, USA). An initial PCR product (~230 bp) amplified using degenerate primers was ligated into a plasmid vector and used to transform *Escherichia coli* cells. Plasmids were purified from each clone and sequenced. Three distinct sequences were obtained that corresponded to the catalytic domain of *G. lateralis GC-Iβ*, *GC-II* and *GC-III*.

5′ RACE and 3′ RACE used the FirstChoice RLM-RACE kits (Applied Biosystems/Ambion, Austin, TX, USA) as described by McDonald et al. (McDonald et al., 2011). Nested primers were used to amplify products from the RACE templates. Outer reactions contained 1 µl 3′ or 5′ RACE template, 2 µl 3′ or 5′ RACE outer primer, 2 µl specific outer primer (supplementary material Table S1), 14.25 µl GoTaq Green mix (Promega) and 30.75 µl nuclease-free water (Integrated DNA Technology). Inner reactions contained 1 µl outer 3′ or 5′ RACE reaction, 1 µl specific inner primer (supplementary material Table S1), 1 µl 3′ or 5′ RACE inner primer, 5 µl GoTaq Green mix (Promega) and 2 µl nuclease-free water. PCR conditions were 3 min denaturation at 94°C, followed by 35 cycles of 30 s at 94°C, 30 s at 60°C, 1 min 30 s at 72°C, and a final extension of 7 min at 72°C. PCR products were separated by 1.0% agarose gel electrophoresis and stained with ethidium bromide. The gel slices were purified using Qiaex II Gel Extraction kit (Qiagen, Valencia, CA, USA) and DNA was ligated into pJet 1.2 (Fermentas) vector, which was transformed into CH3 Blue *E. coli* cells (Bioline USA, Taunton, MA, USA). Plasmids were purified using QIAprep Spin Miniprep kit (Qiagen) and sequenced using pJET sequence-specific primers (Davis Sequencing, Davis, CA, USA). Nested 3′ RACE yielded the remainder of the 3′ open reading frame (ORF) and the 3′ untranslated region (UTR) of *Cm-GC-Iβ* and *Cm-GC-III*. 3′ RACE failed to amplify the complete 3′ sequence of the *Cm-GC-II*. However, a second sequence was obtained when the RLM-RACE kit reverse primer apparently annealed to an A-rich sequence in the kinase homology (KH) domain 5′ to the guanylyl cyclase (GC) domain in the ORF (Table 2). An additional 5′ sequence of *Cm-GC-III* was amplified using sequence-specific *Cm-GC-II* gap bridging primers (supplementary material Table S1). The *Cm-GC-II* primer sequences and *Cm-GC-III* cDNA sequence apparently were similar enough to allow annealing of the primers to the *Cm-GC-III* cDNA. Nested 5′ RACE failed to obtain the 5′ UTR of *Cm-GC-II* and *Cm-GC-Iβ*, which was most likely due to the predicted length (~2100 and ~1600 bp, respectively), based on the *G. lateralis* GC sequences. The DNA and translated amino acid sequences of *GC-Iβ*, *Cm-GC-II* and *Cm-GC-III* were deposited in GenBank.

Acknowledgements
The authors thank Elizabeth Pennock and Stacie Grannum for technical assistance and Kira Marshall, Kent Schnacke and Talia Head for animal care.

Competing interests
The authors declare no competing financial interests.

Author contributions
A.M.A. and D.L.M. conceived the experiments. All authors were involved in the design and execution of the experiments and analysis and interpretation of data. A.M.A., K.S.M., E.S.C. and D.L.M. drafted and revised the article.

Funding
The study was supported by the National Science Foundation (NSF grant IOS-0745224).

Supplementary material
Supplementary material available online at
http://jeb.biologists.org/lookup/suppl/doi:10.1242/jeb.093385/-/DC1

References

Abramowitz, A. A. (1937). The chromatophorotropic hormone of the Crustacea: standardization, properties, and physiology of the eyestalk glands. *Biol. Bull.* **72**, 344-365.
Adelung, D. (1971). Untersuchung zur Häutungsphysiologie der dekapoden Krebse am Beispiel der Strandkrabbe *Carcinus maenas*. *Helgol. Wiss. Meeresunters.* **22**, 66-119.
Andrew, R. D., Orchard, I. and Saleuddin, A. S. M. (1978). Structural re-evaluation of the neurosecretory system in the crayfish eyestalk. *Cell Tissue Res.* **190**, 235-246.
Baghdassarian, D., de Bessé, N., Saïdi, B., Sommé, G. and Lachaise, F. (1996). Neuropeptide-induced inhibition of steroidogenesis in crab molting glands: involvement of cGMP-dependent protein kinase. *Gen. Comp. Endocrinol.* **104**, 41-51.
Bazin, F. (1977a). Effects of injections of ecdysterone on the molt and regeneration in the crab *Carcinus maenas* (L.). *C. R. Acad. Sci.* **284**, 765-768.
Bazin, F. (1977b). Inhibitory effect of ecdysterone on regeneration by the crab *Carcinus maenas* (L.). *C. R. Acad. Sci.* **284**, 1211-1214.
Bliss, D. E. and Welsh, J. H. (1952). The neurosecretory system of brachyuran Crustacea. *Biol. Bull.* **103**, 157-169.
Bliss, D. E., Durand, J. B. and Welsch, J. H. (1954). Neurosecretory systems in decapod Crustacea. *Z. Zellforsch. Mikrosk. Anat.* **39**, 520-536.
Brown, F. A., Jr (1961). Physiological rhythms. In *The Physiology of Crustacea*, Vol. 2 (ed. T. H. Waterman), pp. 401-430. New York, NY: Academic Press.
Buchholz, F. and Adelung, D. (1979). Investigations on the effects of injected ecdysone upon the green shore crab *Carcinus maenas* L. *Z. Naturforsch. C* **34C**, 608-611.
Bückmann, D. and Adelung, D. (1964). Der Einfluss der Umweltfaktoren auf das Wachstum und den Häutungsrhythmus der Strandkrabbe *Carcinides maenas*. *Helgol. Wiss. Meeresunters.* **10**, 91-103.
Carlisle, D. B. (1954). On the hormonal inhibition of moulting in decapod Crustacea. *J. Mar. Biol. Assoc. UK* **33**, 61-63.
Carlisle, D. B. (1957). On the hormonal inhibition of moulting in decapod Crustacea. II. The terminal anecdysis in crabs. *J. Mar. Biol. Assoc. UK* **36**, 291-307.
Carlson, S. P. (1936). Color changes in brachyuran crustaceans, especially in *Uca pugilator*. *Kungl. Fysiograf. Sällskap. Förhandl. Lund* **6**, 63-80.
Chang, E. S. (1989). Endocrine regulation of molting in Crustacea. *Rev. Aquat. Sci.* **1**, 131-157.
Chang, E. S. and Mykles, D. L. (2011). Regulation of crustacean molting: a review and our perspectives. *Gen. Comp. Endocrinol.* **172**, 323-330.
Christie, A. E. (2011). Crustacean neuroendocrine systems and their signaling agents. *Cell Tissue Res.* **345**, 41-67.
Chung, J. S. and Webster, S. G. (2003). Moult cycle-related changes in biological activity of moult-inhibiting hormone (MIH) and crustacean hyperglycaemic hormone (CHH) in the crab, *Carcinus maenas*. From target to transcript. *Eur. J. Biochem.* **270**, 3280-3288.
Chung, J. S., Zmora, N., Katayama, H. and Tsutsui, N. (2010). Crustacean hyperglycemic hormone (CHH) neuropeptidesfamily: functions, titer, and binding to target tissues. *Gen. Comp. Endocrinol.* **166**, 447-454.
Cooke, I. M. and Sullivan, R. E. (1982). Hormones and neurosecretion. In *The Biology of Crustacea*, Vol. 3 (ed. H. L. Atwood and D. C. Sandeman), pp. 206-278. New York, NY: Academic Press.
Covi, J. A., Chang, E. S. and Mykles, D. L. (2009). Conserved role of cyclic nucleotides in the regulation of ecdysteroidogenesis by the crustacean molting gland. *Comp. Biochem. Physiol.* **152A**, 470-477.
Covi, J. A., Bader, B. D., Chang, E. S. and Mykles, D. L. (2010). Molt cycle regulation of protein synthesis in skeletal muscle of the blackback land crab, *Gecarcinus lateralis*, and the differential expression of a myostatin-like factor during atrophy induced by molting or unweighting. *J. Exp. Biol.* **213**, 172-183.
Covi, J. A., Chang, E. S. and Mykles, D. L. (2012). Neuropeptide signaling mechanisms in crustacean and insect molting glands. *Invertebr. Reprod. Dev.* **56**, 33-49.
Crothers, J. H. (1967). The biology of the shore crab *Carcinus maenas* (L.). I. The background – anatomy, growth and life history. *Field Studies* **2**, 407-434.
Darling, J. A., Bagley, M. J., Roman, J., Tepolt, C. K. and Geller, J. B. (2008). Genetic patterns across multiple introductions of the globally invasive crab genus *Carcinus*. *Mol. Ecol.* **17**, 4992-5007.
de Rivera, C. E., Grosholz, E. D. and Ruiz, G. M. (2011). Multiple and long-term effects of an introduced predatory crab. *Mar. Ecol. Prog. Ser.* **429**, 145-155.
Fanjul-Moles, M. L. (2006). Biochemical and functional aspects of crustacean hyperglycemic hormone in decapod crustaceans: review and update. *Comp. Biochem. Physiol.* **142C**, 390-400.
Fingerman, M. (1965). Chromatophores. *Physiol. Rev.* **45**, 296-339.
Geller, J. B., Walton, E. D., Grosholz, E. D. and Ruiz, G. M. (1997). Cryptic invasions of the crab *Carcinus* detected by molecular phylogeography. *Mol. Ecol.* **6**, 901-906.
Goodwin, T. W. (1960). Biochemistry of pigments. In *The Physiology of Crustacea*, Vol. 1 (ed. T. H. Waterman), pp. 101-140. New York, NY: Academic Press.
Grosholz, E. D. (2005). Recent biological invasion may hasten invasional meltdown by accelerating historical introductions. *Proc. Natl. Acad. Sci. USA* **102**, 1088-1091.
Grosholz, E. D. and Ruiz, G. M. (1995). Spread and potential impact of the recently introduced European green crab, *Carcinus maenas*, in Central California. *Mar. Biol.* **122**, 239-247.
Grosholz, E. D. and Ruiz, G. M. (1996). Predicting the impact of introduced marine species: lessons from the multiple invasions of the European green crab *Carcinus maenas*. *Biol. Conserv.* **78**, 59-66.
Grosholz, E. D., Ruiz, G. M., Dean, C. A., Shirley, K. A., Maron, J. L. and Connors, P. G. (2000). The impacts of a nonindigenous marine predator in a California bay. *Ecology* **81**, 1206-1224.
Hänfling, B., Edwards, F. and Gherardi, F. (2011). Invasive alien Crustacea: dispersal, establishment, impact and control. *BioControl* **56**, 573-595.
Hopkins, P. M. (2012). The eyes have it: a brief history of crustacean neuroendocrinology. *Gen. Comp. Endocrinol.* **175**, 357-366.
Jamieson, G. S., Grosholz, E. D., Armstrong, D. A. and Elner, R. W. (1998). Potential ecological implications from the introduction of the European green crab, *Carcinus maenas* (Linneaus), to British Columbia, Canada, and Washington, USA. *J. Nat. Hist.* **32**, 1587-1598.
Jaros, P. P. (1978). Tracing of neurosecretory neurons in crayfish optic ganglia by cobalt iontophoresis. *Cell Tissue Res.* **194**, 297-302.
Kim, H. W., Batista, L. A., Hoppes, J. L., Lee, K. J. and Mykles, D. L. (2004). A crustacean nitric oxide synthase expressed in nerve ganglia, Y-organ, gill and gonad of the tropical land crab, *Gecarcinus lateralis*. *J. Exp. Biol.* **207**, 2845-2857.
Kimbro, D. L., Grosholz, E. D., Baukus, A. J., Nesbitt, N. J., Travis, N. M., Attoe, S. and Coleman-Hulbert, C. (2009). Invasive species cause large-scale loss of native California oyster habitat by disrupting trophic cascades. *Oecologia* **160**, 563-575.
Kingan, T. G. (1989). A competitive enzyme-linked immunosorbent assay: applications in the assay of peptides, steroids, and cyclic nucleotides. *Anal. Biochem.* **183**, 283-289.
Klein, J. M., Mangerich, S., de Kleijn, D. P. V., Keller, R. and Weidemann, W. M. (1993). Molecular cloning of crustacean putative molt-inhibiting hormone (MIH) precursor. *FEBS Lett.* **334**, 139-142.
Kleinholz, L. H. (1961). Pigmentary effectors. In *The Physiology of Crustacea*, Vol. 2 (ed. T. H. Waterman), pp. 133-169. New York, NY: Academic Press.
Lachaise, F., Hubert, M., Webster, S. G. and Lafont, R. (1988). Effect of moult-inhibiting hormone on ketodiol conversion by crab Y-organs. *J. Insect Physiol.* **34**, 557-562.
Lachaise, A., Le Roux, A., Hubert, M. and Lafont, R. (1993). The molting gland of crustaceans: localization, activity, and endocrine control (a review). *J. Crustac. Biol.* **13**, 198-234.
Lee, S. G. and Mykles, D. L. (2006). Proteomics and signal transduction in the crustacean molting gland. *Integr. Comp. Biol.* **46**, 965-977.
Lee, S. G., Bader, B. D., Chang, E. S. and Mykles, D. L. (2007a). Effects of elevated ecdysteroid on tissue expression of three guanylyl cyclases in the tropical land crab *Gecarcinus lateralis*: possible roles of neuropeptide signaling in the molting gland. *J. Exp. Biol.* **210**, 3245-3254.
Lee, S. G., Kim, H. W. and Mykles, D. L. (2007b). Guanylyl cyclases in the tropical land crab, *Gecarcinus lateralis*: cloning of soluble (NO-sensitive and -insensitive) and membrane receptor forms. *Comp. Biochem. Physiol.* **2D**, 332-344.
Lenel, R. and Veillet, A. (1951). Effects de l'ablation des pédoncules oculaires sur les pigments caroténoïdes du crabe *Carcinus maenas*. *C. R. Acad. Sci.* **233**, 1064-1065.
Lu, W., Wainwright, G., Olohan, L. A., Webster, S. G., Rees, H. H. and Turner, P. C. (2001). Characterization of cDNA encoding molt-inhibiting hormone of the crab, *Cancer pagurus*; expression of MIH in non-X-organ tissues. *Gene* **278**, 149-159.
McDonald, A. A., Chang, E. S. and Mykles, D. L. (2011). Cloning of a nitric oxide synthase from green shore crab, *Carcinus maenas*: a comparative study of the effects of eyestalk ablation on expression in the molting glands (Y-organs) of *C. maenas*, and blackback land crab, *Gecarcinus lateralis*. *Comp. Biochem. Physiol.* **158A**, 150-162.
McGaw, I. J. and Naylor, E. (1992). Distribution and rhythmic locomotor patterns of estuarine and open-shore populations of *Carcinus maenas*. *J. Mar. Biol. Assoc. UK* **72**, 599-609.
McGaw, I. J., Kaiser, M. J., Naylor, E. and Hughes, R. N. (1992). Intraspecific morphological variation related to the molt cycle in color forms of the shore crab *Carcinus maenas*. *J. Zool.* **228**, 351-359.
Medler, S., Brown, K. J., Chang, E. S. and Mykles, D. L. (2005). Eyestalk ablation has little effect on actin and myosin heavy chain gene expression in adult lobster skeletal muscles. *Biol. Bull.* **208**, 127-137.

Mykles, D. L. (2001). Interactions between limb regeneration and molting in decapod crustaceans. *Am. Zool.* **41**, 399-406.
Mykles, D. L. (2011). Ecdysteroid metabolism in crustaceans. *J. Steroid Biochem. Mol. Biol.* **127**, 196-203.
Mykles, D. L., Adams, M. E., Gäde, G., Lange, A. B., Marco, H. G. and Orchard, I. (2010). Neuropeptide action in insects and crustaceans. *Physiol. Biochem. Zool.* **83**, 836-846.
Nakatsuji, T. and Sonobe, H. (2004). Regulation of ecdysteroid secretion from the Y-organ by molt-inhibiting hormone in the American crayfish, *Procambarus clarkii*. *Gen. Comp. Endocrinol.* **135**, 358-364.
Nakatsuji, T., Sonobe, H. and Watson, R. D. (2006). Molt-inhibiting hormone-mediated regulation of ecdysteroid synthesis in Y-organs of the crayfish (*Procambarus clarkii*): involvement of cyclic GMP and cyclic nucleotide phosphodiesterase. *Mol. Cell. Endocrinol.* **253**, 76-82.
Nakatsuji, T., Lee, C. Y. and Watson, R. D. (2009). Crustacean molt-inhibiting hormone: structure, function, and cellular mode of action. *Comp. Biochem. Physiol.* **152A**, 139-148.
Pouchet, G. (1872). Sur les rapides changements de coloration provoqués expérimentalement, chez les Crustacés et sur les colorations bleues des poissons. *J. Anat. Physiol.* **8**, 401-407.
Reid, D. G., Abello, P., Kaiser, M. J. and Warman, C. G. (1997). Carapace colour, inter-moult duration and the behavioural and physiological ecology of the shore crab *Carcinus maenas*. *Estuar. Coast. Shelf Sci.* **44**, 203-211.
Saïdi, B., de Bessé, N., Webster, S. G., Sedlmeier, D. and Lachaise, F. (1994). Involvement of cAMP and cGMP in the mode of action of molt-inhibiting hormone (MIH) a neuropeptide which inhibits steroidogenesis in a crab. *Mol. Cell. Endocrinol.* **102**, 53-61.
Shibley, G. A. (1968). Eyestalk function in chromatophore control in a crab, *Cancer magister*. *Physiol. Zool.* **41**, 268-279.
Skinner, D. M. (1985). Molting and regeneration. In *The Biology of Crustacea*, Vol. 9 (ed. D. E. Bliss and L. H. Mantel) pp. 43-146. New York, NY: Academic Press.
Skinner, D. M. and Graham, D. E. (1972). Loss of limbs as a stimulus to ecdysis in Brachyura (true crabs). *Biol. Bull.* **143**, 222-233.
Spindler, K. D., Adelung, D. and Tchernigovtzeff, C. (1974). A comparison of the methods of molt staging according to Drach and to Adelung in the common shore crab, *Carcinus maenas*. *Z. Naturforsch. C* **29**, 754-756.
Stephens, G. C. (1951). A molt-inhibiting factor in the central nervous system of the crayfish, *Cambarus* sp. *Anat. Rec.* **111**, 572-573.
Stewart, M. J., Stewart, P., Sroyraya, M., Soonklang, N., Cummins, S. F., Hanna, P. J., Duan, W. and Sobhon, P. (2013). Cloning of the crustacean hyperglycemic hormone and evidence for molt-inhibiting hormone within the central nervous system of the blue crab *Portunus pelagicus*. *Comp. Biochem. Physiol.* **164A**, 276-290.
Styrishave, B., Rewitz, K. and Andersen, O. (2004a). Frequency of moulting by shore crabs *Carcinus maenas* (L.) changes their colour and their success in mating and physiological performance. *J. Exp. Mar. Biol. Ecol.* **313**, 317-336.
Styrishave, B., Rewitz, K., Lund, T. and Andersen, O. (2004b). Variations in ecdysteroid levels and Cytochrome p_{450} expression during moult and reproduction in male shore crabs *Carcinus maenas*. *Mar. Ecol. Prog. Ser.* **274**, 215-224.
Tamone, S. L., Taggart, S. J., Andrews, A. G., Mondragon, J. and Nielsen, J. K. (2007). The relationship between circulating ecdysteroids and chela allometry in male tanner crabs: evidence for a terminal molt in the genus *Chionoecetes*. *J. Crustac. Biol.* **27**, 635-642.
Tepolt, C. K., Darling, J. A., Bagley, M. J., Geller, J. B., Blum, M. J. and Grosholz, E. D. (2009). European green crabs (*Carcinus maenas*) in the northeastern Pacific: genetic evidence for high population connectivity and current-mediated expansion from a single introduced source population. *Divers. Distrib.* **15**, 997-1009.
Tiu, S. H. K. and Chan, S. M. (2007). The use of recombinant protein and RNA interference approaches to study the reproductive functions of a gonad-stimulating hormone from the shrimp *Metapenaeus ensis*. *FEBS J.* **274**, 4385-4395.
Toullec, J. Y. and Dauphin-Villemant, C. (1994). Dissociated cell suspensions of *Carcinus maenas* Y-organs as a tool to study ecdysteroid production and its regulation. *Experientia* **50**, 153-158.
Webster, S. G. (1986). Neurohormonal control of ecdysteroid biosynthesis by *Carcinus maenas* Y-organs *in vitro*, and preliminary characterization of the putative molt-inhibiting hormone (MIH). *Gen. Comp. Endocrinol.* **61**, 237-247.
Webster, S. G., Keller, R. and Dircksen, H. (2012). The CHH-superfamily of multifunctional peptide hormones controlling crustacean metabolism, osmoregulation, moulting, and reproduction. *Gen. Comp. Endocrinol.* **175**, 217-233.
Zhu, D. F., Hu, Z. H. and Shen, J. M. (2011). Moult-inhibiting hormone from the swimming crab, *Portunus trituberulatus* (Miers, 1876). PCR cloning, tissue distribution, and expression of recombinant protein in *Escherichia coli* (Migula, 1895). *Crustaceana* **84**, 1481-1496.